

## Supporting Information:

### Improved droplet elongation model and value for surface tension of AuSi

*Christopher R. Y. Andersen & Kristian S. Mølhave*

#### Table of Contents

1	Image analysis procedure .....	1
2	Sensitivity analysis of interface and side facets .....	4

#### 1 Image analysis procedure

Each frame from the video provided by Federico Panciera was analyzed using an image analysis procedure in MATLAB 2021b<sup>1</sup> to measure the droplet geometry and the distance between the nanowire and the counter electrode. The analysis involved image rotation, localizing the droplet-nanowire interface, the counter electrode, and the droplet perimeter. The perimeter distance to the models described below was evaluated using the mean squared error (MSE), as described in the following sections. Additionally, the perimeter was fitted to an ellipse for comparison with the analysis done by Panciera et al..<sup>2</sup>

The pixel-to-nanometer scale and the applied bias were the same for each frame as those used in the original analysis by Panciera et al..<sup>2</sup> The conversion factor was 0.7799 nm/pixel; however, the actual image resolution was likely limited to a few nanometers due to the technical constraints of the TEM. A reasonable estimate of the uncertainty from the image analysis can be derived from the interface analysis presented below, where the distance from the center of the fitted sigmoid function to the maximum intensity is approximately 7 nm.

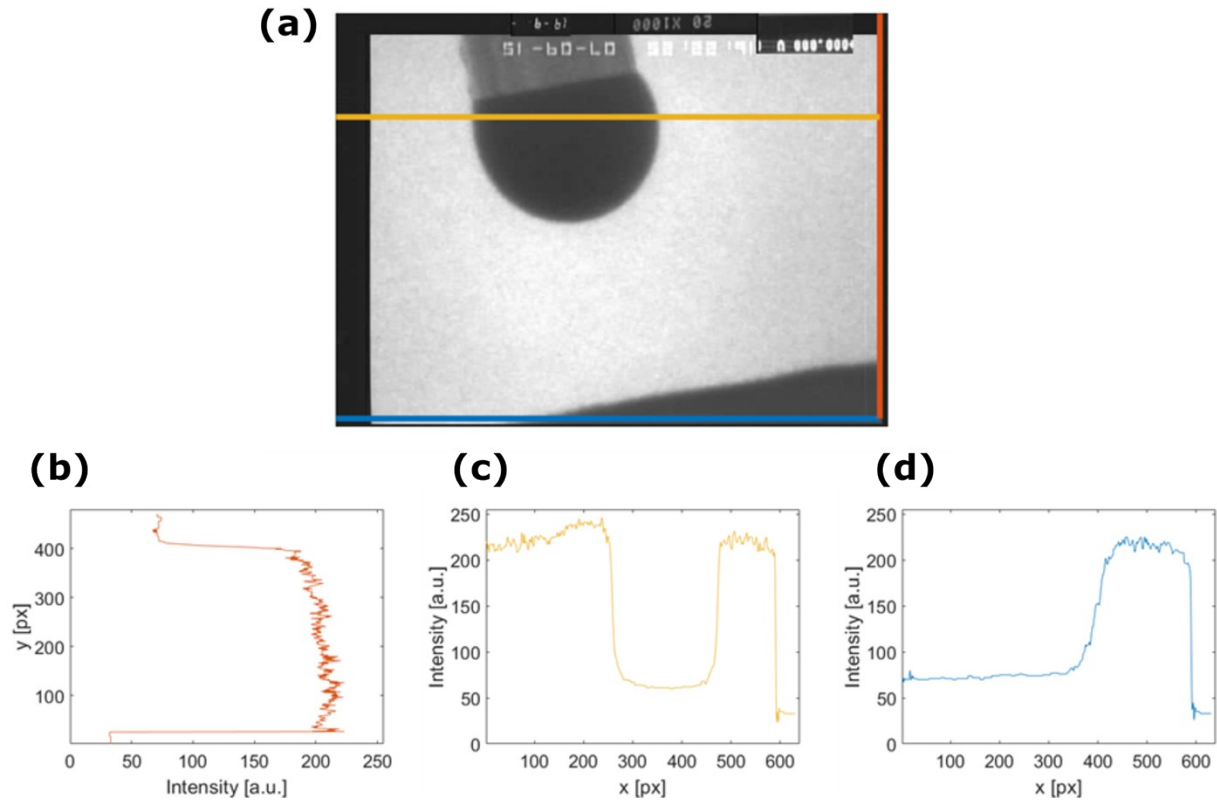


*Fig. S1: Image characteristics illustrated for a frame (a) with line scans along the y-axis (b), and x-axis crossing the droplet (c) and counter electrode (d), respectively.*

The region between the two microcantilevers was imaged, to provide an overview of the distance between the adjacent cantilevers, with the nanowire growing from one and almost reaching the other. These measurements, including the nanowire length and the gap to the neighboring cantilever, were used as inputs for modeling to ensure accurate electric field strength. Video images captured the elongation dynamics of the nanowire as field strength was varied (Fig. S1a). The imaging was performed perpendicular to the nanowire zone axis in the Si  $\langle 110 \rangle$  direction.

Each video frame consisted of 640 x 480 pixels and contained the following segments: Background (Vapor), nanowire (Solid), droplet (Liquid), counter electrode (Solid), and data associated with each frame. The pixel intensity ranged from black to white with values of 0 to 255 with the background (Vapor) ideally around 250. Fluctuations in the individual points, as shown by the red intensity line scan in Fig. S1b, caused slight variations. Inhomogeneous illumination was also present, which is visible as variations in both the vertical (red) and horizontal (yellow) intensity line scans in the vacuum near the droplet (Fig. S1b,c). The droplet, nanowire, and counter electrode were characterized by significant intensity drop, as illustrated in the line scans in Fig. S1b-d, aiding the segmentation process based on intensity.

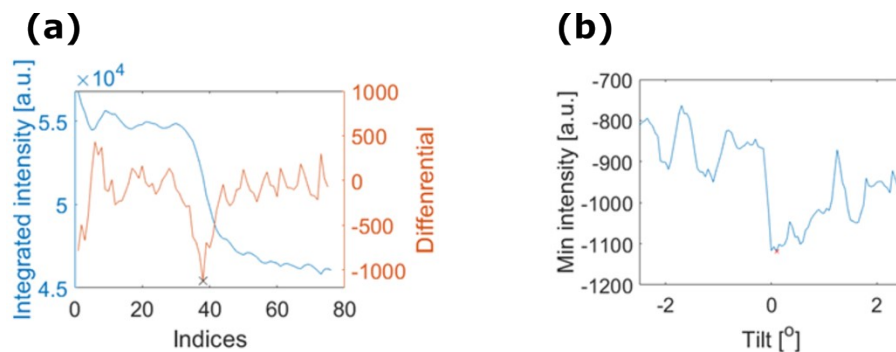


*Fig. S2: Optimization of image rotation based on scans along the nanowire at the droplet-nanowire interface (a). The differential of the integrated intensity is shown on the right-side y-axis with the minimum of this indicated by a black x. Minima at the interface for various image rotations were identified (b) to locate the correct rotation, which corresponds to the lowest minimum.*

**The image was rotated** to align the nanowire interface with the horizontal axis (Fig. S2). Initially, the center of the droplet interface was identified, and an estimated width of the nanowire was used to crop the region around the droplet-nanowire interface. The height of the region of interest was set to 75 pixels to include both a reasonable region of the nanowire and the droplet. An initial rotation of  $170^\circ$  was applied, which served as a preliminary estimate. This was fine-tuned by testing rotations ranging from  $167.5^\circ$  to  $172.5^\circ$  in steps of  $0.05^\circ$ . The region of interest was summed along the x-axis, and the differential was found along the integrated intensity peak, as illustrated for one tilted image in Fig. S2a. The interface was determined as the minimum peak, indicated by a black x in Fig. S2a. The minimum peak for all the rotated images was then found, which is at its minimum when the interface is horizontally aligned as shown in Fig. S2b.

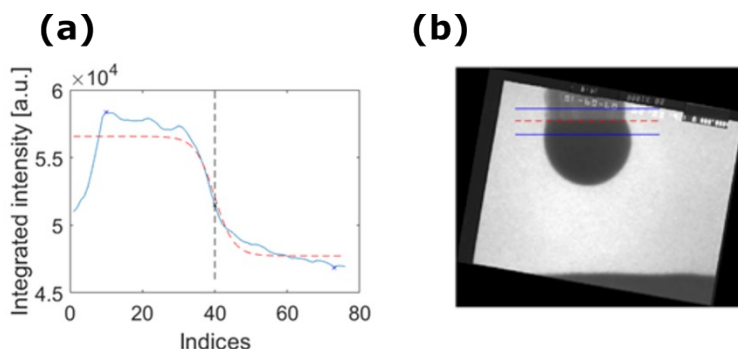


*Fig. S3: (a) The horizontally averaged intensity (blue) as a function of distance along the nanowire axis was fitted to a sigmoid function (red). The center of the sigmoid was used to define the interface between the nanowire and the droplet (black). (b) The region of interest is highlighted in blue, with the identified interface shown in red.*

**The interface between the droplet and nanowire** was determined from the rotated image by fitting the interface transition region with a sigmoid function going from the solid region to the droplet region. The horizontally averaged intensity is shown in Fig. S3a, while the region of interest and the identified interface are illustrated in Fig. S3b.

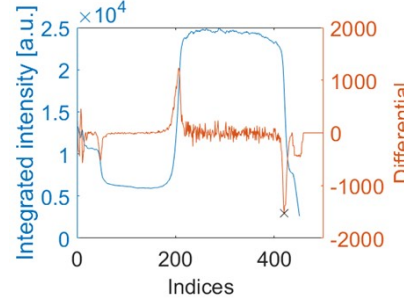


Fig. S4: The integrated intensity from the nanowire interface to the counter electrode. The differential of the horizontally averaged intensity was used to define the counter electrode, with the minimum indicated by a black x.

The **position of the counter electrode** was determined by identifying the minimum in the intensity differential at the transition from vapor to solid, as shown in Fig. S4.

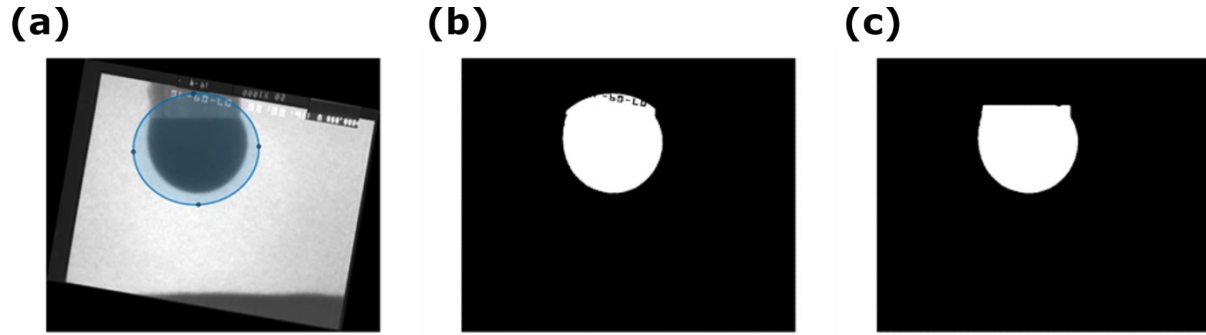


Fig. S5: The region of interest was manually defined by using an ellipsoidal shape (a), and a manually defined threshold value was applied to identify the droplet based on higher intensity (b). Image processing was used to segment the full droplet shape, resulting in the final segmentation (c).

The **droplet perimeter** was determined through image-segmentation within a user-defined region of interest, cropped using an ellipse, as illustrated in Fig. S5a. The droplet area was further defined by a user-defined threshold making a black and white image, as shown in Fig. S5b. Segmentation was done using the image processing tools in Matlab 2021b: *bwareafilt* was used to find the biggest white region, *imdilate* and *imerode* were used for making a smoother shape, holes were then removed using *imfill* and finally, an *imopen*-operation was used to smooth further. The perimeter was extracted using *bwboundaries*. The resulting segmentation is shown in Fig. S5c.

For comparison with the elliptic fitting by Panciera et al. and as input for the finite element model (FEM) geometry, a conic ellipse was fitted using the Least-Squares criterion with zero tilt, based on the function provided by Ohad Gal<sup>3</sup>.

The Mean Squared Error (MSE) was calculated for all the experimental perimeter data points,  $N$ , and the nearest data point from the best-fit ellipse or FEM as

$$r_i^2 = (x_{fit,i} - x_{exp,i})^2 + (y_{fit,i} - y_{exp,i})^2 \quad \text{Eqn. S1}$$

$$MSE = \sum_i \frac{r_i^2}{N}$$

Eqn. S2

The results of the elliptic fit analysis for a single frame are shown in Fig. S6.

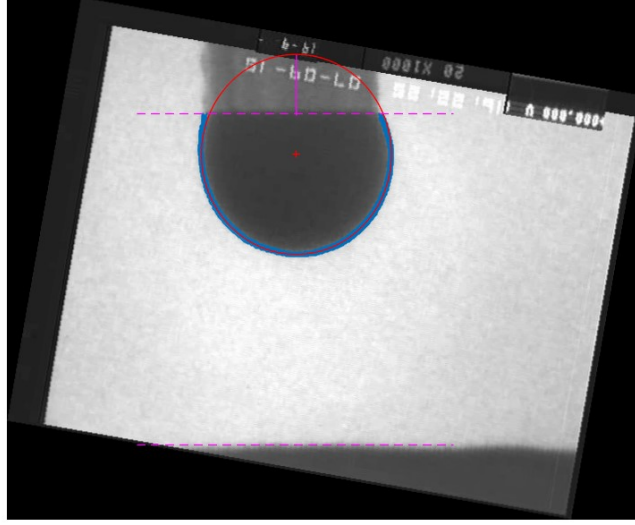


*Fig. S6: The analysis results showing the droplet perimeter (blue), the best-fit ellipse (red), and the nanowire interface and counter electrode (dashed magenta lines).*

## 2 Sensitivity analysis of interface and side facets

The droplet-nanowire interfaces are shown in Fig. S7a-c, along with the region of interest at the interface (Fig. S7d-f) and the normalized integrated intensity (Fig. S7h-j). A decrease in the integrated intensity would be expected if the edge was beveled. Some variation (Fig. S7h-j) near the left-hand side edge may suggest instability at the droplet-nanowire interface. However, this variation is more likely to appear from the sawtooth edge itself, which is visible on the left-hand side and as described elsewhere.<sup>4</sup> Additionally, the poor resolution of the images presents an important source of error for this analysis.

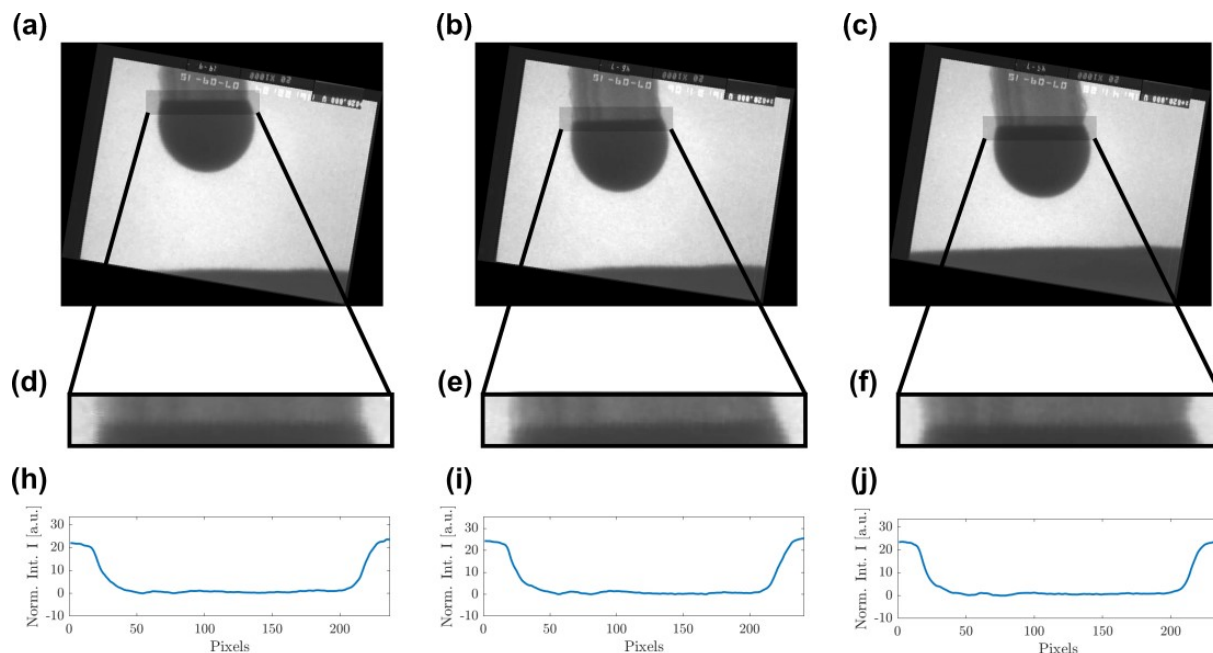
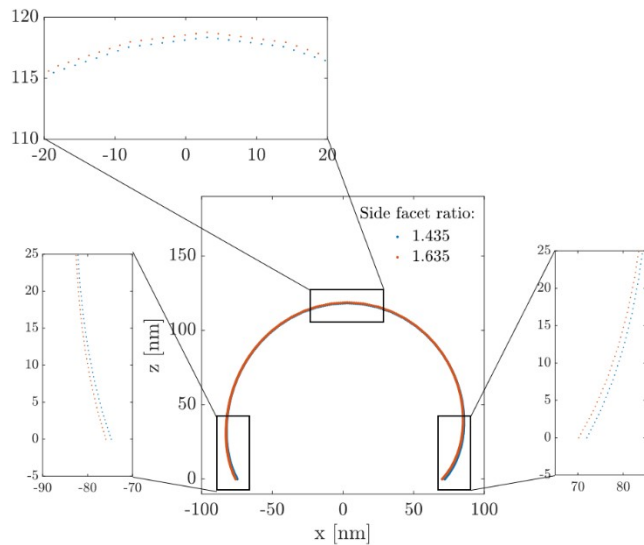
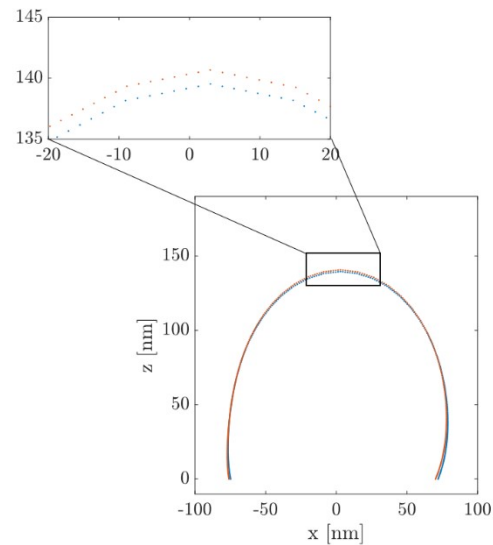


*Fig. S7: The droplet-nanowire interfaces are shown for three droplets at an applied field of 1V for the three distances examined in the main text (a-c), respectively. The corresponding regions of interest for these three images are shown (d-f), and the normalized integrated intensity at each pixel along the interface is plotted (h-j).*

The effect of the side facet on the droplet shape is discussed in the main text and the results of this analysis are provided in Fig. S8. The droplet was simulated with side facet ratios of  $\pm 0.1$ . The height differences for the droplet perimeters were found to be 0.4 nm and 1.1 nm at 1 V and 101V, respectively, corresponding to differences of 0.6% and 0.8%. These results indicate that varying the side facet ratio within its reported uncertainty does not significantly affect the droplet shape compared to changes in surface tension<sup>5, 5</sup>. However, besides fitting the volume of the model to the data, the side facet could have been adjusted to achieve a slightly better match between the experimental observations and simulations.



(a) 1V



(b) 101V

Fig. S8: The droplet was simulated with side facet ratios of  $1.535 \pm 0.1$  at two different biases: 1V (a) and 101V (b).

## References

- 1 MATLAB (R2021b), Natick, Massachusetts: The MathWorks Inc., 2022.
- 2 F. Panciera, M. M. Norton, S. B. Alam, S. Hofmann, K. Mølhave and F. M. Ross, *Nat Commun*, 2016, **7**, 12271.
- 3 O. Gal, 2023, fit\_ellipse, [https://www.mathworks.com/matlabcentral/fileexchange/3215-fit\\_ellipse](https://www.mathworks.com/matlabcentral/fileexchange/3215-fit_ellipse), MATLAB Central File Exchange. Retrieved September 15, 2023.
- 4 F. M. Ross, J. Tersoff and M. C. Reuter, *Phys Rev Lett*, 2005, **95**, 146104.
- 5 J. M. Bae, W. J. Lee, J. W. Ma, J. H. Kim, S. H. Oh, M. H. Cho, K. Chul, S. Jung and J. Park, *J Mater Chem C Mater*, 2015, **3**, 2123–2131.